A&A 365, 258–265 (2001)
DOI: 10.1051/0004-6361:20000330

Astronomy & Astrophysics

Atomic data from the IRON project

XLVI. Electron excitation of $3s3p^6$ and $3s^23p^43d$ fine-structure transitions in Fe x

J. C. Pelan[2] and K. A. Berrington[1]

[1] School of Science & Mathematics, Sheffield Hallam University, Sheffield S1 1WB, UK
[2] Gatsby Computational Neuroscience Unit, University College, 17 Queen Square, London WC1N 3AR, UK

Received 21 July 2000 / Accepted 2 October 2000

Abstract. Electron excitation collision strengths for fine-structure transitions $3s^23p^5$–$3s3p^6$, $3s^23p^5$–$3s^23p^43d$ and $3s3p^6$–$3s^23p^43d$ in Fe x, are calculated using a 180-level Breit-Pauli R-matrix calculation containing the above levels together with those from $3s3p^53d$ and $3s^23p^33d^2$ configurations. The collision strength is averaged over a Maxwellian velocity distribution to obtain the effective fine-structure collision strengths as a function of electron temperature from $\log T(\mathrm{K}) = 5.4-7.0$. We show that low-energy resonances enhance the effective collision strength, with significant effects on level populations.

Key words. atomic data

1. Introduction

The astrophysical significance of chlorine-like iron (Fe x) cannot be over-stated. Its lines are observed in many kinds of astronomical phenomena, from novae to cool stars, and so it plays an important role in modelling stellar atmospheres including that of the sun. In fact much interest stems from efforts to determine the precise mechanisms behind the origin of the solar wind using corona diagnostics. This has created much demand for accurate collisional data which this paper aims to address.

Previous collisional work on this ion include several distorted-wave (DW) calculations, including Blaha (1968, 1969), Krueger & Czyzak (1970), Nussbaumer & Osterbrock (1970), Mason (1975), Davis et al. (1976), Malinivsky et al. (1980), Mann (1983) and Bhatia & Doschek (1995). Some of these authors only calculated collision strengths for a few transitions, and in a previous paper in the IRON project series (Pelan & Berrington 1995) we compared new R-matrix calculations for $3s^23p^5\ {}^2\mathrm{P}^{\mathrm{o}}_{3/2}$–${}^2\mathrm{P}^{\mathrm{o}}_{1/2}$ with data from these sources. Mason also tabulated excitation data to the lowest 31 levels (i.e. from $3s^23p^5$ to the $3s3p^6$ and $3s^23p^43d$ levels), and Bhatia and Doschek tabulated collisonal data among 54 levels (i.e. including also the $3s3p^53d$ levels), giving the collision strength for a few medium-to-high energies. However, resonance structure is not normally included in these DW calculations, and we show in the present paper that this can have a significant effect on the calculated rates for excited transitions. Since Bhatia and Doschek give a good review of the earlier data, we confine ourselves in this paper to comparisons with them.

R-matrix calculations include the IRON project work of Pelan & Berrington (1995) on the ground-state fine-structure transition in Cl-like ions. R-matrix methods include resonances and channel coupling effects, and typically more target states are included in the model atom than just the required initial and final states, in order to obtain the effect of resonance structures converging to higher levels. Pelan and Berrington included the lowest 14 LS terms (i.e. all $3s^23p^5$, $3s3p^6$ and $3s^23p^43d$ terms), and used an algebraic transformation to intermediate coupling (Saraph 1978). Mohan et al. (1994) also reported a similar R-matrix calculation, however their calculation appeared to omit some resonance contributions and this was discussed more fully by Pelan and Berrington.

The present calculation is part of an international collaboration known as the IRON Project (Hummer et al. 1993), and extends the R-matrix calculation of Pelan & Berrington (1995) to tabulate data for Fe x from the lowest three levels to the lowest 31 levels. 180 target

Send offprint requests to: K. A. Berrington

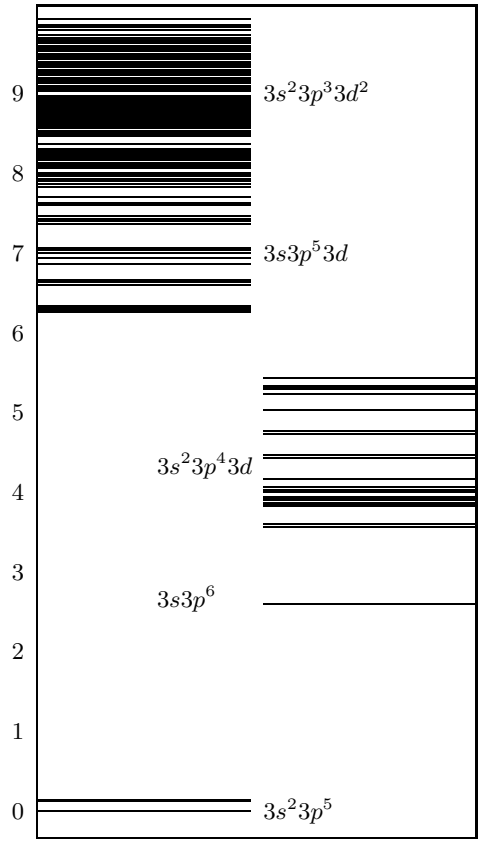

Fig. 1. The model atom: calculated energies (Ryds) of the 180 levels from the 75 terms included for Fe X

levels were actually included in the present R-matrix calculation, arising from $3s^23p^5$, $3s3p^6$, $3s^23p^43d$, $3s3p^53d$ and $3s^23p^33d^2$ configurations, as shown in Fig. 1. A full Breit-Pauli R-matrix (BPRM) treatment was adopted because term mixing among the $3s^23p^43d$ levels was considered too big for the algebraic transformation to be valid. This 180-level BPRM calculation is the biggest so far on this ion: the collision calculation required the setting up and diagonalizing of Hamiltonian matrices of order 6164, with 1104 coupled channels.

2. The calculation

The basic atomic theory, the approximations and the computer codes employed in the IRON Project are described by Hummer et al. (1993). The target wavefunctions were constructed from 1s, 2s, 2p, 3s and 3p orbitals as given by Clementi & Roetti (1974), together with a 3d orbital optimised on the energy of the third $^2P^{\rm o}$ state (i.e. $3s3p^53d$), and a 4f correlation orbital optimised on the ground state. The optimizations were carried out using Hibbert's (1975) variational program CIV3. The radial parts of the Slater-type orbitals are

$$\begin{aligned} 3{\rm d}(r) \;=\; & 141.9677864\exp(-8.0582535r)r^3 \\ & +58.2199125\exp(-4.3181676r)r^3 \end{aligned}$$

$$4{\rm f}(r) \;=\; 183.85325\exp(-5.175)r^4.$$

All configurations were included with a minimum number of electrons in each shell of $1s^22s^22p^63s^03p^2$ and with a maximum of three electrons in the 3d shell and one electron in 4f. This correlation was necessary in order to converge the oscillator strength for the $3s^23p^5$–$3s3p^6$ transitions. Two complementary R-matrix calculations were carried out, as now described.

A 180-level BPRM calculation was used for the resonance energy region (up to 9.95 Ryd), with a maximum of 1104 channels in each partial wave. In order for this calculation to be computational feasable, the number of continuum terms was the minimum required to span this energy range: only five per channel, resulting in collisional Hamiltonian matrices of maximum order 6164. The purpose of this calculation was to obtain accurate collision strengths in the low-energy resonance region, and since resonances are important only for low partial waves the expansion was truncated at $J = 6$.

A 31-level BPRM calculation was used to top-up both the energy and the partial-wave expansion, in order to calculate converged collision strengths to a high enough energy for collision rates to be obtained over a realistic temperature range. The 31-level calculation had only 158 channels, so 30 continuum terms per channel could be included and the partial-waves calculated up to $J = 56$, enabling converged collision strengths to be calculated for the transitions $3s^23p^5$–$3s3p^6$, $3s^23p^5$–$3s^23p^43d$ and $3s3p^6$–$3s^23p^43d$ (i.e. up to the lowest 31 levels), and the energy range extended from 9.95 to 600 Ryd.

Table 1 lists the energies of the lowest 31 levels calculated from the wavefunction used in the 181-level BPRM calculation, and compares with NIST reference data. Table 2 compares the oscillator strengths obtained using the 181-level BPRM wavefunction with those of Bhatia & Doshek (1995). The oscillator strengths from the two calculations are qualitatively similar but not in very good agreement. However, our results are much closer to a recent experiment by Träbert (1996) for the lifetime and branching ratio of the $3s3p^6\ ^2S^{\rm e}_{1/2}$ level (Table 3).

3. Results

We calculated collision strengths Ω for fine-structure transitions $3s^23p^5$–$3s3p^6$, $3s^23p^5$–$3s^23p^43d$ and $3s3p^6$–$3s^23p^43d$. In Table 4 we show a limited comparison with earlier work, the DW calculation of Bhatia & Doschek (1995), at energies above all thresholds. (Note that they also give data at 9 Ryd, and make a comparison with Mason (1975) at 5.5 Ry, but we cannot meaningfully compare at these low energies because of resonances, see Fig. 1.) Generally the agreement is reasonably good for excitations to level 4 and above ($3s^23p^43d$ levels), but rather poorer for the $3s^23p^5$–$3s3p^6$ doublet, the latter may be explained by the difference in calculated oscillator strength between the two calculations, as summarised in Table 3.

Table 1. The lowest 31 energy levels (Ryd) for Fe X. For reference, level 32 ($3s3p^5 3d$) is calculated at 6.284 Ryd. 180 levels were actually included in the calculation (see Fig. 1). "Expt" is reference data from Sugar & Corliss (1985)

i	State	J	Present	Expt
1	$3s^2 3p^5$	$^2P^o$ 3/2	.0000	.0000
2	$3s^2 3p^5$	$^2P^o$ 1/2	.1346	.1429
3	$3s3p^6$	$^2S^e$ 1/2	2.631	2.636
4	$3p^4 3d$	$^4D^e$ 5/2	3.581	3.542
5	$3p^4 3d$	$^4D^e$ 7/2	3.582	3.542
6	$3p^4 3d$	$^4D^e$ 3/2	3.591	3.554
7	$3p^4 3d$	$^4D^e$ 1/2	3.603	3.568
8	$3p^4 3d$	$^4F^e$ 9/2	3.863	3.806
9	$3p^4 3d$	$^2P^e$ 1/2	3.875	
10	$3p^4 3d$	$^4F^e$ 7/2	3.906	3.853
11	$3p^4 3d$	$^4F^e$ 5/2	3.938	3.889
12	$3p^4 3d$	$^4F^e$ 3/2	3.947	3.903
13	$3p^4 3d$	$^2P^e$ 3/2	3.952	3.936
14	$3p^4 3d$	$^4P^e$ 1/2	4.014	3.962
15	$3p^4 3d$	$^2D^e$ 3/2	4.015	3.961
16	$3p^4 3d$	$^4P^e$ 3/2	4.057	
17	$3p^4 3d$	$^4P^e$ 5/2	4.079	4.026
18	$3p^4 3d$	$^2F^e$ 7/2	4.081	4.017
19	$3p^4 3d$	$^2D^e$ 5/2	4.097	
20	$3p^4 3d$	$^2G^e$ 9/2	4.172	4.108
21	$3p^4 3d$	$^2G^e$ 7/2	4.173	4.111
22	$3p^4 3d$	$^2F^e$ 5/2	4.195	4.126
23	$3p^4 3d$	$^2F^e$ 5/2	4.460	
24	$3p^4 3d$	$^2F^e$ 7/2	4.495	4.429
25	$3p^4 3d$	$^2D^e$ 3/2	4.735	4.664
26	$3p^4 3d$	$^2D^e$ 5/2	4.774	
27	$3p^4 3d$	$^2S^e$ 1/2	5.059	4.938
28	$3p^4 3d$	$^2P^e$ 3/2	5.255	5.141
29	$3p^4 3d$	$^2P^e$ 1/2	5.307	5.194
30	$3p^4 3d$	$^2D^e$ 5/2	5.351	5.221
31	$3p^4 3d$	$^2D^e$ 3/2	5.466	5.342

Figures 2 to 4 show some illustrative plots of the calculated collision strength at low scattering energies. All these transitions are affected by resonances in the first 2 or 3 Rydbergs above threshold: these resonances arise primarily from the $3s^2 3p^4 3d$ states, with resonances arising

Table 2. gf-values for transitions from the $3p^5\ ^2P^o_{3/2,1/2}$ ground levels to the the $3s3p^6$ and $3p^4 3d$ levels for Fe X. BD = gf calculated by Bhatia & Doshek (1995); Present = gf calculated from the same wavefunction as used in the present 181-level BPRM collision calculation; A = present calculated A-value, s^{-1}. The level indexing (i, i') is defined in Table 1

i–i'	$J_{i'}$	BD	Present	A, s^{-1}
1–3	1/2	0.0716	0.1027	2.854E9
1–4	5/2	0.71E-4	2.08E-4	3.504E6
1–6	3/2	2.06E-4	2.02E-4	5.281E6
1–7	1/2	9.14E-5	5.59E-5	2.926E6
1–9	1/2	2.68E-3	8.12E-4	4.954E7
1–11	5/2	1.24E-3	1.49E-3	3.031E7
1–12	3/2	19.7E-3	9.03E-3	2.783E8
1–13	3/2	5.65E-5	2.10E-3	6.651E7
1–14	1/2	2.25E-3	3.56E-3	2.325E8
1–15	3/2	9.56E-3	4.85E-3	1.557E8
1–16	3/2	28.2E-4	4.17E-4	1.397E7
1–17	5/2	6.40E-3	4.64E-3	1.017E8
1–19	5/2	15.9E-3	3.67E-3	8.114E7
1–22	5/2	11.1E-4	6.82E-4	1.579E7
1–23	5/2	3.66E-3	4.60E-3	1.206E8
1–25	3/2	0.0131	0.0100	4.441E8
1–26	5/2	0.58E-3	2.45E-3	7.356E7
1–27	1/2	1.940	1.312	1.338E11
1–28	3/2	3.788	2.817	1.542E11
1–29	1/2	0.1863	0.3693	4.260E10
1–30	5/2	6.462	5.128	1.941E11
1–31	3/2	0.283	0.1710	1.013E10
2–3	1/2	0.0365	0.0513	1.285E9
2–6	3/2	31.9E-6	2.93E-6	7.094E4
2–7	1/2	13.6E-5	7.75E-5	3.757E6
2–9	1/2	72.0E-3	3.62E-3	2.055E8
2–12	3/2	7.51E-3	3.96E-3	1.137E8
2–13	3/2	4.16E-4	3.95E-4	1.169E7
2–14	1/2	6.77E-4	7.17E-4	4.382E7
2–15	3/2	8.56E-3	3.31E-3	9.929E7
2–16	3/2	15.9E-5	6.84E-5	2.149E6
2–25	3/2	11.7E-3	7.62E-3	3.193E8
2–27	1/2	0.2115	0.4553	4.403E10
2–28	3/2	0.2402	0.1052	5.468E9
2–29	1/2	1.833	1.091	1.196E11
2–31	3/2	4.004	3.213	1.810E11

Table 3. Predictions and measurement (Träbert 1996) on the line doublet $3s^2 3p^5\ ^2P^o_{3/2,1/2}$– $3s3p^6\ ^2S^e_{1/2}$ for Fe X. BD = calculated from Bhatia & Doshek (1995); Present = calculated from the same wavefunction as used in the present 181-level BPRM collision calculation

	BD	Present	Measured
Lifetime ps.	344	242	270 ± 20
Branch ratio	2.17	2.22	2.4 ± 0.3

Table 4. A comparison of collision strengths for Fe X fine structure transitions as a function of electron impact energy (Ryd). The level indexing (i, i') is defined in Table 1; the numbers on the same line as the transition are collision strengths from the present calculation and the ones below labelled BD are from Bhatia & Doschek (1995) for the same transition

i–i'	18.0	27.0	36.0	45.0
1–3	.356	.363	.361	.361
BD	.421	.441	.461	.479
2–3	.186	.188	.188	.188
BD	.226	.239	.252	.262
1–4	.044	.028	.020	.015
BD	.039	.026	.018	.013
2–4	.014	.0085	.0060	.0045
BD	.012	.0079	.0056	.0042
3–4	.0020	.0013	.0010	.0008
BD	.0020	.0013	.0009	.0007
1–5	.0662	.0423	.0293	.0213
BD	.0593	.0383	.0265	.0193

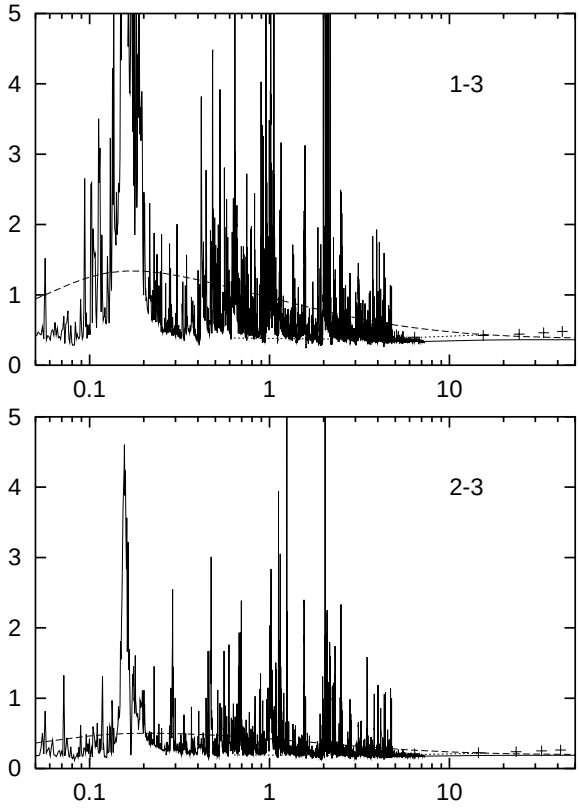

Fig. 2. Collision strength for $3s^2 3p^5\ ^2P^o_{3/2,1/2}$–$3s3p^6\ ^2S^e_{1/2}$ (1–3 and 2–3) in Fe X, as a function of electron energy (Ryds) relative to threshold: —, Ω from the present 180-level BPRM calculation; - - - -, the resulting thermal average (Υ) plotted against kT in Ryds; . . . . ., Υ from Mohan et al. (1994); + + +, Ω from Bhatia & Doschek (1995)

from the $3s3p^5 3d$ and higher states having negligible effect on transitions from the ground state (Figs. 2, 3). However, Fig. 4 show significant resonance structure up to 6 Ryd above threshold for excitation out of the $3s3p^6$ initial state, and this justifies the inclusion of the $3s3p^5 3d$ and higher levels in the 180-level BPRM calculation in order to obtain accurate data for these transitions.

Collision strengths are computed for the required fine-structure transitions over a sufficiently wide and fine energy mesh in order to be able to integrate over a Maxwellian distribution to obtain the *effective collision strength* Υ, from which the excitation and de-excitation rate coefficients can easily be obtained (Hummer et al. 1993). Our energy mesh was determined by increasing the number of points until the integration converged: resulting in an energy spacing of 0.001–0.002 Ryd in the resonance regions, a total of 7460 energy points. The range of temperatures chosen was $\pm$ 0.8 dex of the temperature of maximum ionic abundance given by Shull & Van Steenberg (1982), and our final results are tabulated in Table 6.

Our effective collision strengths Υ are also plotted in Figs. 2–4 as a function of kT Rydbergs, alongside the collision strength Ω: the figures illustrate that the enhancement of Υ due to low-energy resonances extends to surprisingly large temperatures ($\sim 10^6$ K). Typical enhancements are factors of two or three for transitions from the ground state (Figs. 2–3) and up to an order of magnitude for the optically forbidden transitions out of the excited $3s3p^6$ level (Fig. 4).

For comparison we also plot the DW Ω from Bhatia & Doshek (1995) and the early R-matrix calculation of Υ of Mohan et al. (1994), showing that although our present results agree well with these at higher energies (see also Table 4), these other calculations appear to underestimate or ignore the resonance contribution at low temperatures.

To see the effect of the resonance enhancement more clearly, we recalculate in Table 5 the level populations given by Bhatia & Doschek (1995) for electron density

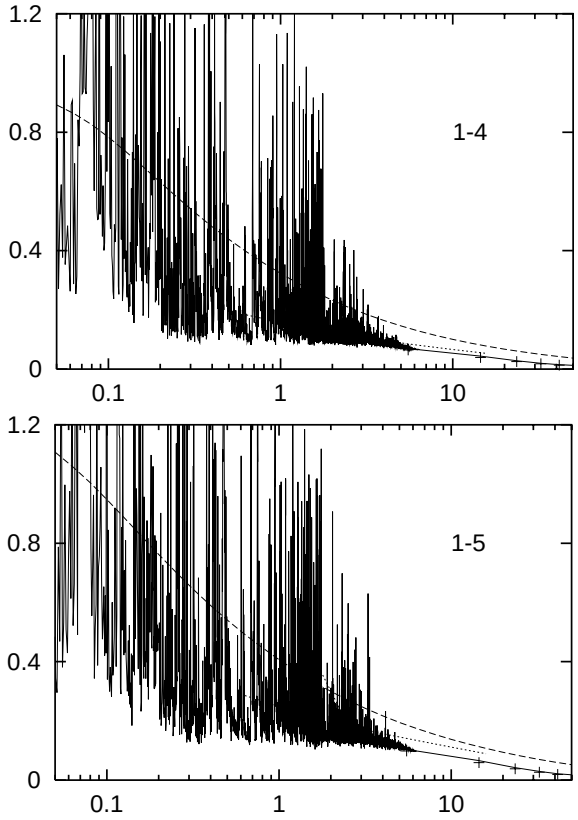

Fig. 3. Collision strength for $3s^2 3p^5\ {}^2P^o_{3/2}$–$3s^2 3p^4 3d\ {}^4D^e_{5/2,7/2}$ (1–4 and 1–5) in Fe X, as a function of electron energy relative to threshold: notation as in Fig. 2

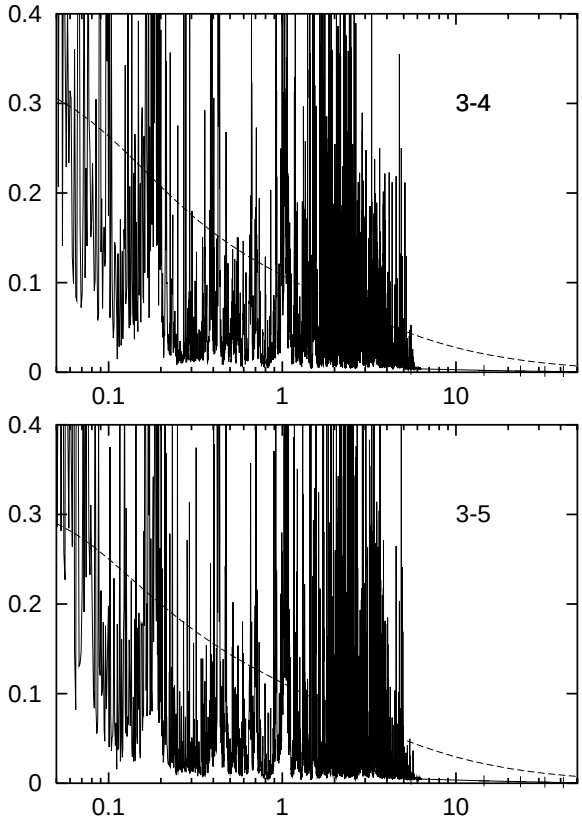

Fig. 4. Collision strength for $3s 3p^6\ {}^2S^e_{1/2}$–$3s^2 3p^4 3d\ {}^4D^e_{5/2,7/2}$ (3–4 and 3–5) in Fe X, as a function of electron energy relative to threshold: notation as in Fig. 2

Table 5. Effect of resonances on the derived level populations for Fe X. "BD" is from Table IV A of Bhatia & Doschek (1995) for electron density 10^{10} cm^{-3} and 10^6 K. "Present" substitutes our rates from Tables 2 & 6 for those of BD

i	BD	Present	i	BD	Present
1	7.23E-01	6.19E-01	17	1.16E-08	1.31E-08
2	1.36E-01	1.73E-01	18	1.97E-02	1.55E-02
3	1.86E-09	1.39E-09	19	5.36E-09	1.31E-08
4	1.46E-06	3.70E-07	20	1.31E-02	1.28E-02
5	2.92E-02	4.10E-02	21	1.33E-02	1.05E-02
6	1.03E-07	1.19E-07	22	5.67E-08	4.48E-08
7	2.30E-08	4.43E-08	23	1.02E-08	6.11E-09
8	4.24E-02	8.68E-02	24	4.81E-03	3.88E-03
9	1.14E-09	1.66E-09	25	5.37E-10	5.73E-10
10	1.86E-02	3.69E-02	26	3.81E-08	7.29E-09
11	4.11E-08	3.09E-08	27	8.40E-11	7.83E-11
12	2.18E-08	1.90E-09	28	1.65E-10	3.25E-12
13	1.72E-09	6.33E-09	29	3.88E-11	4.92E-11
14	1.11E-09	1.85E-09	30	2.23E-10	2.08E-10
15	2.30E-09	2.16E-09	31	6.26E-11	7.48E-11
16	7.91E-09	3.32E-08			

10^{10} cm^{-3} and 10^6 K, with no proton excitation or blackbody radiative excitation. We use all our radiative and collisonal rates from Tables 2 and 6 (i.e. for transitions involving levels 1, 2 and 3), and complete the dataset up to level 31 using Bhatia and Doschek's data: the rate equations are then solved as in their Eq. (3) for the level populations. Our resonance-enhanced Υ for 1–2 ($^2P_{3/2-1/2}$), which we published in an earlier IP paper (Pelan & Berrington 1995), gives some redistribution of population between level 1 and 2. But the total ^{2}P ground population drops 7% when the Υ from the ground state to higher levels also includes resonances as in the present work, and the population of $^4F_{9/2}$ and $^4F_{7/2}$ (levels 8 and 10 in Table 5) doubles.

Thus, we conclude that it is not safe to calculate rates from earlier tabulations of the collision strength without taking into account resonance enhancement. We believe that, by including resonance structure associated with 180 levels, we have included the most significant resonance effects on transitions to the 31 lowest levels.

Acknowledgements. This work was done with the support of a PPARC grant GR/K97608. We would like to thank Drs. P. Young and H. Mason for providing the level populations code.

Table 6. Effective collision strengths for Fe X fine structure transitions as a function of $\log T$ (Kelvin). The level indexing (i, i') is defined in Table 1. (The 1–2 data is from Pelan & Berrington 1995)

i–i'	5.4	5.6	5.8	6.0	6.2	6.4	6.6	6.8	7.0
1–2	2.97	2.69	2.27	1.79	1.35	0.99	0.73	0.54	0.40
1–3	0.7939	0.6812	0.5868	0.5133	0.4602	0.4241	0.4008	0.3867	0.3792
1–4	0.1742	0.1496	0.1262	0.1045	0.0849	0.0674	0.0522	0.0394	0.0291
1–5	0.2389	0.2063	0.1755	0.1468	0.1203	0.0963	0.0749	0.0566	0.0415
1–6	0.0993	0.0856	0.0722	0.0597	0.0484	0.0384	0.0298	0.0226	0.0168
1–7	0.0418	0.0360	0.0304	0.0250	0.0201	0.0158	0.0121	0.0091	0.0067
1–8	0.1702	0.1480	0.1252	0.1036	0.0839	0.0664	0.0514	0.0390	0.0291
1–9	0.0715	0.0625	0.0523	0.0428	0.0349	0.0284	0.0232	0.0189	0.0154
1–10	0.1281	0.1097	0.0913	0.0744	0.0595	0.0469	0.0368	0.0291	0.0234
1–11	0.0846	0.0722	0.0599	0.0488	0.0391	0.0308	0.0239	0.0184	0.0141
1–12	0.1132	0.1001	0.0863	0.0729	0.0606	0.0500	0.0411	0.0340	0.0286
1–13	0.0697	0.0603	0.0507	0.0419	0.0338	0.0264	0.0199	0.0146	0.0105
1–14	0.0944	0.0814	0.0682	0.0573	0.0480	0.0392	0.0311	0.0241	0.0185
1–15	0.0792	0.0729	0.0661	0.0574	0.0476	0.0380	0.0295	0.0225	0.0169
1–16	0.0543	0.0469	0.0394	0.0329	0.0283	0.0255	0.0240	0.0232	0.0228
1–17	0.1343	0.1209	0.1065	0.0930	0.0816	0.0726	0.0659	0.0611	0.0580
1–18	0.1351	0.1206	0.1054	0.0907	0.0785	0.0699	0.0648	0.0625	0.0621
1–19	0.1619	0.1375	0.1140	0.0953	0.0820	0.0732	0.0676	0.0644	0.0629
1–20	0.1627	0.1438	0.1257	0.1100	0.0974	0.0882	0.0823	0.0793	0.0787
1–21	0.1177	0.0995	0.0815	0.0650	0.0507	0.0387	0.0289	0.0211	0.0150
1–22	0.1101	0.0933	0.0768	0.0622	0.0500	0.0403	0.0330	0.0277	0.0241
1–23	0.1045	0.0891	0.0758	0.0648	0.0560	0.0493	0.0447	0.0420	0.0409
1–24	0.1288	0.1096	0.0943	0.0822	0.0728	0.0661	0.0622	0.0608	0.0614
1–25	0.0580	0.0530	0.0489	0.0453	0.0425	0.0406	0.0394	0.0388	0.0386
1–26	0.0594	0.0526	0.0473	0.0435	0.0416	0.0415	0.0424	0.0437	0.0450
1–27	1.908	1.917	1.925	1.933	1.939	1.943	1.950	1.963	1.982
1–28	3.856	3.870	3.898	3.934	3.966	3.992	4.018	4.053	4.101
1–29	0.4783	0.4762	0.4802	0.4924	0.5122	0.5362	0.5608	0.5839	0.6047
1–30	6.805	6.883	6.963	7.032	7.083	7.124	7.171	7.236	7.323
1–31	0.2161	0.2216	0.2240	0.2274	0.2363	0.2512	0.2690	0.2863	0.3018
2–3	0.3508	0.3111	0.2762	0.2481	0.2274	0.2131	0.2039	0.1985	0.1958
2–4	0.0596	0.0504	0.0418	0.0342	0.0274	0.0216	0.0166	0.0125	0.0092
2–5	0.0539	0.0444	0.0358	0.0284	0.0222	0.0170	0.0127	0.0093	0.0067
2–6	0.0532	0.0460	0.0389	0.0324	0.0264	0.0210	0.0163	0.0122	0.0090
2–7	0.0321	0.0283	0.0244	0.0206	0.0170	0.0137	0.0108	0.0082	0.0061
2–8	0.0292	0.0240	0.0192	0.0151	0.0116	0.0088	0.0066	0.0048	0.0034
2–9	0.0312	0.0282	0.0249	0.0216	0.0183	0.0150	0.0118	0.0090	0.0067
2–10	0.0498	0.0424	0.0352	0.0286	0.0227	0.0177	0.0136	0.0105	0.0082
2–11	0.0539	0.0461	0.0385	0.0314	0.0251	0.0196	0.0151	0.0114	0.0085
2–12	0.0787	0.0692	0.0588	0.0484	0.0386	0.0299	0.0226	0.0169	0.0127
2–13	0.0468	0.0399	0.0329	0.0271	0.0228	0.0200	0.0184	0.0173	0.0166
2–14	0.0360	0.0313	0.0262	0.0216	0.0175	0.0138	0.0106	0.0079	0.0057
2–15	0.0308	0.0270	0.0232	0.0194	0.0156	0.0122	0.0093	0.0070	0.0051
2–16	0.0516	0.0453	0.0386	0.0327	0.0285	0.0258	0.0240	0.0227	0.0216

Table 6. continued

$i-i'$	5.4	5.6	5.8	6.0	6.2	6.4	6.6	6.8	7.0
2–17	0.0471	0.0399	0.0329	0.0266	0.0212	0.0166	0.0128	0.0096	0.0070
2–18	0.0866	0.0710	0.0568	0.0452	0.0357	0.0275	0.0205	0.0149	0.0106
2–19	0.0757	0.0677	0.0592	0.0503	0.0424	0.0362	0.0317	0.0284	0.0260
2–20	0.0924	0.0798	0.0677	0.0563	0.0458	0.0364	0.0281	0.0211	0.0154
2–21	0.1118	0.0979	0.0852	0.0745	0.0661	0.0600	0.0561	0.0542	0.0539
2–22	0.0845	0.0726	0.0608	0.0501	0.0411	0.0339	0.0285	0.0247	0.0222
2–23	0.0642	0.0544	0.0458	0.0392	0.0348	0.0328	0.0325	0.0334	0.0352
2–24	0.0611	0.0532	0.0467	0.0414	0.0370	0.0337	0.0316	0.0308	0.0309
2–25	0.0381	0.0343	0.0304	0.0261	0.0215	0.0168	0.0125	0.0090	0.0062
2–26	0.0447	0.0399	0.0356	0.0316	0.0276	0.0238	0.0207	0.0183	0.0167
2–27	0.6641	0.6596	0.6610	0.6714	0.6911	0.7169	0.7446	0.7714	0.7961
2–28	0.1400	0.1386	0.1371	0.1393	0.1488	0.1646	0.1828	0.1999	0.2147
2–29	1.520	1.530	1.540	1.548	1.551	1.550	1.549	1.553	1.564
2–30	0.0292	0.0267	0.0242	0.0219	0.0197	0.0178	0.0162	0.0150	0.0142
2–31	4.289	4.335	4.386	4.431	4.462	4.481	4.500	4.533	4.583
3–4	0.0732	0.0606	0.0474	0.0351	0.0250	0.0173	0.0118	0.0079	0.0053
3–5	0.0749	0.0621	0.0486	0.0361	0.0259	0.0180	0.0123	0.0083	0.0055
3–6	0.0572	0.0480	0.0380	0.0285	0.0204	0.0142	0.0096	0.0064	0.0043
3–7	0.0337	0.0296	0.0244	0.0188	0.0137	0.0095	0.0065	0.0043	0.0028
3–8	0.0452	0.0356	0.0268	0.0193	0.0134	0.0090	0.0060	0.0039	0.0025
3–9	0.1418	0.1254	0.1036	0.0795	0.0575	0.0397	0.0266	0.0175	0.0113
3–10	0.0435	0.0347	0.0263	0.0189	0.0131	0.0088	0.0058	0.0038	0.0025
3–11	0.0400	0.0320	0.0243	0.0176	0.0123	0.0084	0.0057	0.0038	0.0026
3–12	0.1864	0.1659	0.1386	0.1074	0.0783	0.0545	0.0368	0.0245	0.0161
3–13	0.0519	0.0426	0.0332	0.0245	0.0174	0.0119	0.0080	0.0053	0.0034
3–14	0.0768	0.0657	0.0523	0.0395	0.0287	0.0203	0.0141	0.0098	0.0068
3–15	0.0655	0.0568	0.0471	0.0367	0.0270	0.0191	0.0132	0.0091	0.0063
3–16	0.0578	0.0521	0.0435	0.0338	0.0250	0.0181	0.0132	0.0099	0.0077
3–17	0.0858	0.0739	0.0599	0.0463	0.0347	0.0257	0.0193	0.0148	0.0118
3–18	0.0880	0.0722	0.0561	0.0417	0.0299	0.0209	0.0143	0.0097	0.0065
3–19	0.0956	0.0817	0.0659	0.0506	0.0383	0.0296	0.0240	0.0206	0.0186
3–20	0.0776	0.0654	0.0523	0.0398	0.0292	0.0209	0.0147	0.0103	0.0073
3–21	0.0742	0.0599	0.0463	0.0343	0.0245	0.0171	0.0117	0.0080	0.0055
3–22	0.0670	0.0558	0.0437	0.0322	0.0227	0.0154	0.0103	0.0067	0.0044
3–23	0.0485	0.0409	0.0325	0.0245	0.0177	0.0123	0.0084	0.0056	0.0037
3–24	0.0481	0.0401	0.0328	0.0259	0.0196	0.0142	0.0099	0.0067	0.0045
3–25	0.0415	0.0376	0.0328	0.0282	0.0241	0.0208	0.0184	0.0166	0.0154
3–26	0.0521	0.0470	0.0419	0.0372	0.0331	0.0298	0.0273	0.0256	0.0244
3–27	0.2772	0.2710	0.2328	0.1819	0.1331	0.0930	0.0632	0.0422	0.0280
3–28	0.1967	0.1746	0.1408	0.1057	0.0754	0.0520	0.0351	0.0234	0.0154
3–29	0.1179	0.1042	0.0839	0.0629	0.0449	0.0309	0.0208	0.0138	0.0091
3–30	0.1712	0.1370	0.1046	0.0772	0.0558	0.0398	0.0283	0.0203	0.0146
3–31	0.1199	0.0960	0.0736	0.0545	0.0396	0.0285	0.0205	0.0149	0.0110

References

Berrington, K. A., Eissner, W., & Norrington P. H. 1995, Comput. Phys. Commun., 92, 290

Bhatia, A. K., & Doschek G. A. 1995, Atom. Data Nucl. Data Tables, 60, 97

Blaha, M. 1968, Ann. Astrophys., 31, 311

Blaha, M. 1969, A&A, 1, 42

Clementi, E., & Roetti, C. 1974, Atom. Data Nucl. Data Tables, 14, 177

Davis, J., Kepple, P. C., & Blaha, M. 1976, J. Quant. Spectrosc. Radiat. Transfer, 16, 1043

Hibbert, A. 1975, Comput. Phys. Commun., 9, 141

Hummer, D. G., Berrington, K. A., Eissner, W., et al. 1993, A&A, 279, 298 (Paper I)

Krueger, T. K., & Czyzak, S. J. 1970, Proc. R. Soc. London Ser. A, 318, 531

Malinovsky, M., Dubau, J., & Sahal-Brechot, S. 1980, ApJ, 235, 665

Mann, J. B. 1983, At. Data Nucl. Data Tables, 29, 407

Mason, H. E. 1975, MNRAS, 170, 651

Mason, H. E. 1992, Atom. Data Nucl. Data Tables, 57, 305

Mohan, M., Hibbert, A., & Kingston, A. E. 1994, ApJ, 434, 389

Nussbaumer, H., & Osterbrock, D. E. 1970, ApJ, 161, 811

Pelan, J., & Berrington, K. A. 1995, A&AS, 110, 209

Saraph, H. E. 1978, Comp. Phys. Commun., 15, 247

Sugar, J., & Corliss, C. 1985, J. Phys. Chem. Ref. Data, 14 (Suppl. 2), 473

Shull, J. M., & Van Steenberg, M. 1982, ApJS, 48, 95

Träbert, E. 1996, J. Phys. B: At. Mol. Opt. Phys., 29, L217